Experimental characterization of the compatibility between bitumen and fillers from a perspective of bitumen components and filler characteristics

Jiaqiu Xu[1,2], Zepeng Fan[1], Dawei Wang[*1, 3], Zhen Leng[2], Guoyang Lu[4], Pengfei Liu[3]

1. School of Transportation Science and Engineering, Harbin Institute of Technology, Huanghe Road 73, Harbin 150090, China.

2. Department of Civil and Environmental Engineering, The Hong Kong Polytechnic University, Kowloon, Hong Kong, China.

3. Institute of Highway Engineering, RWTH Aachen University, Mies-van-der-Rohe-Straße 1, 52074 Aachen, Germany.

4. Department of Architecture and Civil Engineering, City University of Hong Kong, Kowloon, Hong Kong, China.

**Corresponding author:*

Prof. Dawei Wang, School of Transportation Science and Engineering, Harbin Institute of Technology, Harbin 150090, PR China; Institute of Highway Engineering, RWTH Aachen University, Mies-van-der-Rohe-Street 1, 52074 Aachen, Germany; E-mail addresses: wang@isac.rwth-aachen.de.

Abstract: In the composite system of asphalt mixtures, asphalt mastic, which is composed of fillers and bitumen, plays a key role. To achieve precise control and prediction of the performance of asphalt mastics, the effects of filler characteristics and bitumen components on the performance of mastics were investigated in this study. Five bitumen sources and five filler types were selected to prepare twenty-five kinds of asphalt mastics, and the macro and micro tests were conducted on the mastics. The grey relational analysis (GRA) was applied to quantify the relationship between raw material characteristics and mastic performances. The results indicate that the properties of asphalt mastics exhibit a high correlation with the raw material characteristics. The resin content of bitumen is suggested to be one of the most influential properties for the fatigue performance of asphalt mastics. The penetrations, resins

and aromatics contents of bitumen exhibit a specific contribution to the low-temperature performance of mastics. Among all filler characteristics, D10 (the particle diameter when the pass rate of the filler is 10%) and P20 (the content of fillers with a diameter of less than 0.02mm) are recommended as two critical indicators for selecting fillers because these two parameters exhibit a higher correlation than other similar parameters. The filler characteristics such as particle size and specific surface area significantly affect the fatigue performance of asphalt mastics because the effect of fillers on the fatigue performance of mastics is the competitive mechanism between physical hardening and particle-filling enhancement. This study provides a reference for achieving the better performance of asphalt mastics by controlling bitumen sources and filler characteristics.

Keywords: *Asphalt mastics; Bitumen components; Filler characteristics; Compatibility; Grey relational analysis; Mechanical properties*

1. Introduction

1.1. Key role of asphalt mastics in asphalt mixture composite

From 2016 to 2020, the highway maintenance funds of China accumulated 56.6 billion US dollars [1]. Therefore, the main challenge facing the field of road engineering is how to prolong the durability of asphalt pavements, thus reducing maintenance and improving the service life of pavements. Asphalt mixtures are typical multiphase and heterogeneous composite materials consisting of aggregates with various sizes, shapes, and random orientations embedded in the bitumen matrix [2, 3]. According to modern mortar theory, the asphalt mixture is a three-level spatial network dispersion system [4, 5]. Asphalt mastic is the primary dispersion system in which fillers are dispersed in the bitumen matrix [6]. Next, the asphalt mortar is the second dispersion system in which fine aggregates are distributed in the asphalt mastic matrix. Finally, the asphalt mixture is the third dispersion system in which coarse aggregates are dispersed in the asphalt mortar matrix [7]. In the asphalt mixture system, the asphalt mastic composed of bitumen and fillers plays the role of bonding aggregates rather than the bitumen matrix [8].

There is no doubt that asphalt mastic is the critical component in determining the durability and service performance of asphalt pavements [9, 10]. However, the importance of asphalt mastics has yet to be reflected in the design of asphalt mixtures. The current design criteria mainly specify the performance of the bitumen, and there are few specifications specifying the performance of asphalt mastics. The reason is that there are still many problems to be solved in the research field of asphalt mastics, and the mechanical properties of asphalt mastics need to be accurately predicted and controlled. Undoubtedly, the performance of the asphalt mastic depends mainly on the properties of its constituents, i.e., bitumen and fillers. However, when the combination of the bitumen and filler is not appropriate, the asphalt mastic consisting of the bitumen and filler with excellent properties may exhibit less performance. This study refers to this scientific issue as the compatibility of bitumen and fillers. Specifically, the properties of fillers, such as particle size distribution, mineral composition, SSA, surface morphology, etc., and properties of the bitumen, such as component differences, may be the key factors affecting the mechanical properties of asphalt mastics. Therefore, it is necessary to investigate the compatibility of bitumen and fillers to improve the durability and service life of asphalt mixtures.

1.2. Macroscopic and microscopic studies of asphalt mastics

So far, researchers have carried out lots of experimental studies on asphalt mastics from the macro and micro scales. Cheng [11] et al. selected four fillers with different characteristics, finding that the SSA of filler is the most critical factor affecting the performances of asphalt mastics. The research of Nazary [12] et al. prepared asphalt mastics with three penetration grades of bitumen and three fillers and found that zeolite has better high-temperature properties and limestone has better low-temperature properties through ANOVA analysis. The study of Shukry [13] et al. showed that diatomite has the most significant improvement in the high-temperature performance of modified bitumen and attributed it to the high silica content in diatomite using multiple stress creep recovery (MSCR) test. Li [14] et al. proposed a modified MSCR test for asphalt mastics and investigated the effect of filler on the rutting performance of bitumen. The research of Jiang [15] et al. designed an improved LAS test, combined with the morphology analysis of scanning electron microscope (SEM), to study the impact of the concentration and particle size of fillers on the fatigue performance of asphalt mastics. It can be seen from the above that the filler characteristics have a potential impact on many properties of asphalt mastics, such as rutting, fatigue, low-temperature cracking, and anti-aging. In addition, there were part of researchers putting forward the test methods of asphalt mastics based on the bitumen test methods by increasing the load levels [14, 15]. Nevertheless, these studies did not lead to broad consensus or standardized tests. The more common option is that the researchers still tested the asphalt mastics entirely according to the bitumen test method.

The macro viscoelastic properties and complex rheological behavior of the asphalt mastic depend primarily on its microstructure and morphology, and researchers have also conducted much research on this. In terms of microstructure, the study of Tan [16] et al. studied the interaction between bitumen and fillers using the Fourier transform infrared spectroscopy (FTIR), finding that the interaction between bitumen and fillers was mainly physical action and the disappearance of individual peaks corresponded to weak chemical action. The research of Zhang [17] et al. investigated the microscopic characteristics of asphalt mastics and found no chemical reaction between bitumen and fillers. Xu [18] et al. found that the peak area of sulfoxide of limestone asphalt mastic was larger than diabase and granite asphalt mastics because limestone had the most substantial interaction with bitumen. The research of Li [19] et al. investigated the aging resistance of bitumen through the FTIR test, finding that fillers can enhance the anti-aging performance of bitumen, and fly ash showed the most substantial enhancing effect because of its porous surface. Moraes [20] et al. also found that the use of fillers can effectively slow down the aging of bitumen. To conclude, the existing research shows that the interaction between mineral fillers and bitumen is mainly a physical process.

In terms of morphology, the work of Xing [21, 22] et al. studied the effects of filler particle size on the fatigue of asphalt mastics based on scanning electron microscope (SEM), finding that the fatigue performance of asphalt mastics prepared by coarse particle filler was worse. The research of Xu [18] et al. captured the SEM results of three asphalt mastics, finding that the existence of rich folds and protrusions of limestone can effectively increase the contact area with bitumen and thus increase the adhesion ability. Tan [23] et al. adopted Atomic Force Microscope (AFM) to characterize the morphological characteristics and mechanical properties of asphalt binder at different distances from the filler surface. The research of Fischer [24] et al. used AFM to study the interface interaction between bitumen and fillers and found that the decisive factor was the porosity of the filler.

It can be seen from the above that many studies have been conducted to investigate the effects of raw material characteristics on the performances of asphalt mastics. However, there are still some areas for improvement in the current research. Firstly, the past studies mostly focused on the characteristics of fillers, while neglecting the research on the properties of bitumen such as bitumen components and penetration grades. Secondly, previous studies have not accurately established the relationship between the performances of asphalt mastics and the raw material characteristics of bitumen and filler. For example, to ensure that a good fatigue resistance of the asphalt mastic, it is still unknown which component of the bitumen or which characteristic of the filler should be focused on. It is currently difficult to achieve the goal of controlling the performances of asphalt mastics by controlling the bitumen origins and the filler characteristics.

1.3. Objectives

The objective of this study is to investigate the compatibility between bitumen and fillers from a perspective of bitumen components and filler characteristics and to determine which components of base bitumen and which characteristics of filler have the most contribution to various performances of asphalt mastics. Given this, five bitumen sources and five filler types were selected to prepare twenty-five kinds of asphalt mastics. Macro tests and micro tests were conducted to investigate the performances of mastics on multiple scales. The GRA was adopted to establish the relational degree between raw material characteristics and performances of mastics. This work provides a fundamental understanding of achieving better performance of asphalt mastics by controlling bitumen origins and filler characteristics.

2. Materials and Methods

2.1. Materials

2.1.1. Bitumen

To investigate the effects of the origins, penetration grades, and component differences of the base bitumen on the performance of asphalt mastics, five base bitumen (A, B, C, D, and E) with five sources and three penetration grades (60/70, 70/80, and 90/100) were selected in this study. Table 1 lists the basic properties of five base bitumen. The performance grade (PG) was tested according to AASHTO M 320-21, and the SARA (Saturates, Aromatics, Resins, and Asphaltenes) fractions were tested, referring to ASTM D4124-09.

Table 1. Basic properties of the base bitumen

Properties		A	B	C	D	E
PG (°C)	High PG	66.68	65.35	66.42	69.48	66.86
	Low PG	-22.98	-22	-21.85	-29.41	-30.72
Penetration at 25 °C (0.1 mm)		62.2	68.4	66.5	76.2	93.9
SARA fractions (%)	Saturates	12.78	11.12	31.11	8.00	10.99
	Aromatics	40.78	47.96	30.53	37.73	31.45
	Resins	30.06	25.63	24.13	47.17	50.43
	Asphaltenes	16.38	15.29	14.23	7.10	7.13

2.1.2. Fillers

Five types of fillers were selected in this study. As a considerable amount of solid waste, the application of steel slag as filler in asphalt pavement has gained some attention [25, 26]. In addition, cement is increasingly widely used as a filler in asphalt pavement due to the excellent moisture resistance and aging resistance of cement as a substitute for limestone powder [27-29]. Therefore, steel slag powder and cement were also selected in addition to three mineral fillers (granite, basalt, and limestone). Table 2 lists the basic properties of the fillers used in this study. In the table, SSA refers to the specific surface area of fillers. D10, D50, and D90 refer to the corresponding particle diameter when the pass rate of the filler is 10%, 50% 90%. P20, P10, and P5 refer to the content of fillers with a diameter of less than 0.02 mm, 0.01mm, and 0.005mm, respectively. More parameters of the filler, such as P45 and P75, were not included, which is because the values of these parameters for fillers were all 100%. In addition, the contents of the two main components (SiO_2 and CaO) in the mineral composition of the fillers are also listed in Table 2. Besides, Table 2 also presents the volume fractions of each filler. In this study, the bitumen-filler mass ratio for all asphalt mastics was fixed to 1:1. It is worth noting that the difference between the volume fractions of different fillers under the same bitumen-filler mass ratio is not significant. Considering that this study has set enough variables (25 kinds of asphalt mastics), the impact of different volumetric concentrations of fillers on compatibility is not the focus of this study.

Table 2. Basic properties of the fillers

Characteristics	Granite	Basalt	Limestone	Steel slag	Cement
Density (g/cm^3)	2.673	2.874	2.696	3.19	3.045
SSA (m^2/kg)	252.0	238.2	308.5	477.6	335.8
D10 (μm)	3.48	3.77	3.00	2.66	2.90
D50 (μm)	16.20	17.18	10.63	5.79	9.38

D90 (μm)	25.62	25.80	23.62	8.68	22.42
P20 (%)	65.64	63.13	77.58	100	84.05
P10 (%)	34.03	30.33	47.34	98.08	53.27
P5 (%)	15.49	13.39	21.88	41.17	24.86
SiO_2 (%)	67.39	40.57	2.68	22.00	15.98
CaO (%)	3.08	8.99	74.61	29.54	50.00
Volume fraction (%)	28.20	26.76	28.03	24.76	25.64

2.1.3. Preparation of asphalt mastics

First, the filler sieved through the 0.075mm standard sieve was put into an oven at the temperature of 145°C for two hours to evaporate the potential moisture, and base bitumen was put into an oven at the temperature of 145°C for one hour. Second, the filler was slowly added into the bitumen in several small portions for mixing. The mixing temperature was 150°C, the shear rate was 1000rpm, and the shear time was 0.5h. Until there was no obvious bubble in the mastic, it indicated that a uniformly dispersed asphalt mastic had been prepared. Finally, the asphalt mastic was quickly poured into a sealed aluminum tank and stored for use. It is worth mentioning that, to prevent the precipitation of the filler caused by the long storing time of the asphalt mastic, the asphalt mastic must be stirred evenly before each sampling.

2.2. Micro test methods

2.2.1. Fourier transform infrared spectroscopy (FTIR)

To detect the potential chemical reactions between the bitumen and fillers, the Nicolet iS50 Fourier Transform Infrared Spectrometer manufactured by Thermo Scientific Company of USA was adopted to conduct the FTIR test on the fillers, base bitumen, and asphalt mastics used in this study. For each sample, the tests were repeated three times. FTIR tests of bitumen and asphalt mastics adopted attenuated total reflection (ATR) mode, and tests of fillers adopted transmission mode of FTIR. The ATR mode does not require additional treatment for test sample, while the transmission mode needs to adopt the potassium bromide (KBr) disc method for sample preparation, and the detailed steps can refer to the research of Usman et al [30].

2.2.2. Scanning electron microscopy (SEM)

The microscopic surface morphology of the fillers was characterized by the Merlin Compact field emission scanning electron microscopy (SEM) produced by Carl Zeiss Company of Germany. Before the test, the filler samples were sprayed with a thin layer of gold to enhance the conductivity of the samples.

2.3. Macro test methods

2.3.1. Multiple stress creep recovery (MSCR) test

The rutting factor parameter (G/sinδ) composed of complex modulus (G) and phase angle (δ) was not adopted in this study to evaluate the high-temperature performance of asphalt mastics. It is because G/sinδ is a parameter of materials in the linear viscoelastic range, it reflects the mechanical properties of materials in a non-damaged state [31]. The MSCR test was carried out according to AASHTO TP 70 to characterize the high-temperature damage performance of asphalt mastics by DSR (DHR-2, TA Company, USA). The rolling thin-film oven (RTFO) procedure was performed on the samples before the test, and the test temperature was 60°C.

2.3.2. Linear amplitude sweep (LAS) test

Like the rutting factor, the fatigue factor (G*sinδ) is also a parameter that characterizes the mechanical properties of materials in a non-damaged state, and has no strong correlation with the fatigue cracking of asphalt pavement [32]. Thus, the LAS test was conducted according to AASHTO TP 101-12 to indicate the medium-temperature damage performance of asphalt mastics by DSR (DHR-2, TA Company, USA). The RTFO and pressurized aging vessel (PAV) procedures were performed on the samples before the test, and the test temperature was 25°C.

2.3.3. Bending beam rheometer (BBR) test

To characterize the low-temperature cracking performance of asphalt mastics, the BBR test was carried out according to ASTM D6648-08 by the TE-BBR manufactured by Cannon Instrument Company of the USA. Before the BBR test, the RTFO and PAV procedures were performed on the samples, and three thin beams (127 ± 2 mm × 12.7 ± 0.05 mm × 6.35 ± 0.05 mm) were manufactured, and two test temperatures were set for each kind of asphalt mastic.

2.3.4. Boiling water test

Referring to ASTM D3625M-12, the boiling water test was carried out on asphalt mastics to evaluate the adhesion performance between the asphalt mastic and the coarse aggregates. At first, the coarse aggregates with the size of 13.2~19 mm were selected for testing. The aggregates were cleaned with distilled water and dried for use. Secondly, 10g asphalt mastic and 100g aggregates were mixed evenly at the test temperature of 155°C. Thirdly, the mixture was immediately put into the slightly boiling distilled water to boil for 10 minutes. After the water was cooled to room temperature, the moisture resistance of the asphalt mastic was determined by comparing the peeling of the asphalt mastic on the aggregate surface. It is highly subjective to judge the peeling of the asphalt mastic by visual inspection, which would lead to inaccurate results. Therefore, this study employed a high-definition digital camera to photograph the asphalt mastic after the boiling water test. The professional image analysis software Image-Pro Plus was used to calculate the peeling rate of the asphalt mastic.

2.4. Grey relational analysis (GRA)

GRA is a multi-factor statistical method that obtains the gray correlation degree by processing the sample data of different factors [33]. It can describe the strength of the correlation degree between other factors, and the detailed procedures of GRA are as follows [33, 34]:

(1) Determine the reference sequence X_0 and the comparison sequence X_p:

$$X_0^* = \left\{X_0^*(1), X_0^*(2), ..., X_0^*(N)\right\} \tag{1}$$

$$X_p^* = \left\{X_p^*(1), X_p^*(2), ..., X_p^*(N)\right\} \tag{2}$$

(2) Calculate the dimensionless sequences of X_0 and X_p.

(3) Calculate the difference between the dimensionless series:

$$\Delta_i(k) = \left|x_0(k) - x_i(k)\right|, (k = 1, 2, 3, ..., n) \tag{3}$$

(4) Determine the maximum and minimum of the sequence differences:

$$\Delta_{\max} = \max_i \max_k \Delta_i(k), \Delta_{\min} = \min_i \min_k \Delta_i(k) \tag{4}$$

(5) Calculate the correlation coefficient $\gamma_{0i}(k)$:

$$\gamma_{0i}(k)=\frac{\Delta\min+\rho\Delta\max}{\Delta_i(k)+\rho\Delta\max} \tag{5}$$

Where ρ is the resolution factor, which is usually equal to 0.5.

(6) Calculate the grey relational degree γ_{0i}:

$$\gamma_{0i}=\frac{1}{n}\sum_{k=1}^{n}\gamma_{0i}(k) \tag{6}$$

Where n is the length of the comparison sequences. A higher γ_{0i} indicates that the sequences $X_i(k)$ and $X_0(k)$ are more strongly related.

3. Results and discussion

3.1. Microscopic test results

3.1.1. FTIR test results

Figure 1a shows the FTIR test results of five fillers used in the study. First, the characteristic peaks at 1425 cm^{-1}, 876 cm^{-1}, and 712 cm^{-1} are the absorption peaks of CaO. Limestone has significant absorption peaks at these three places, and steel powder and cement have significant absorption peaks at 1425 cm^{-1} and 876 cm^{-1}, which indicates that one of the constituents of these fillers is calcium carbonate ($CaCO_3$). Secondly, the characteristic peaks at 1097 cm^{-1} and 1008 cm^{-1} are the anti-symmetric stretching vibration peaks of Si-O-Si. Granite has significant absorption peaks at 1097 cm^{-1} and 1008 cm^{-1}, basalt and steel powder have peaks at 1008 cm^{-1}, and cement at 1097 cm^{-1}. In addition, the characteristic peak at 514 cm^{-1} is the symmetric stretching vibration peak of the Si-O bond, which can be found in granite, basalt, steel powder, and cement.

Figure 1b ~ 1d show the FTIR test results of asphalt mastics based on bitumen A. Because the laws observed from the FTIR test results of the five types of base bitumen are consistent, this part only takes bitumen A as an example. From the figures, the FTIR test results between the fillers and bitumen can be divided into two categories. The first category is mineral fillers, including granite, basalt, and limestone. For these three fillers, it can be seen from the figure that some new functional groups do appear on the FTIR curves of the asphalt mastic compared to that of the bitumen. For example, two new characteristic peaks can be found in the FTIR curves of A+Limestone at 876 cm^{-1} and 712 cm^{-1}, and two new characteristic peaks can be found in A+Granite at 1097 cm^{-1} and 1008 cm^{-1}. However, combined with the FTIR results of the fillers above, it is not difficult to see that these functional groups are native to the filler. It can be concluded that no prominent new characteristic peaks independent of bitumen and filler are observed in the asphalt mastics, indicating that the interaction between the bitumen and these three fillers is mainly physical adsorption, and there is no significant chemical reaction. The second category includes steel slag and cement. From the figures, three are also functional groups from the fillers found in the FTIR curves of the asphalt mastics, such as the characteristic peaks in the FTIR curves of A+Steel slag and A+Cement at 514 cm^{-1}. More importantly, it is found that the sulfoxide group (S=0 at 1030 cm^{-1}) in the base bitumen cannot be found in the FTIR curves of these two asphalt mastics (A+Steel slag and A+Cement). Thus, it is easy to infer that these strong alkaline fillers (steel slag and cement) produce chemical reactions with the acid group (sulfoxide group) in the base bitumen. According to previous literature, the products formed by the chemical reaction above have extremely firm adhesion [35, 36]. It is foreseeable that adding steel slag and cement will significantly improve the adhesion properties between the bitumen and aggregates.

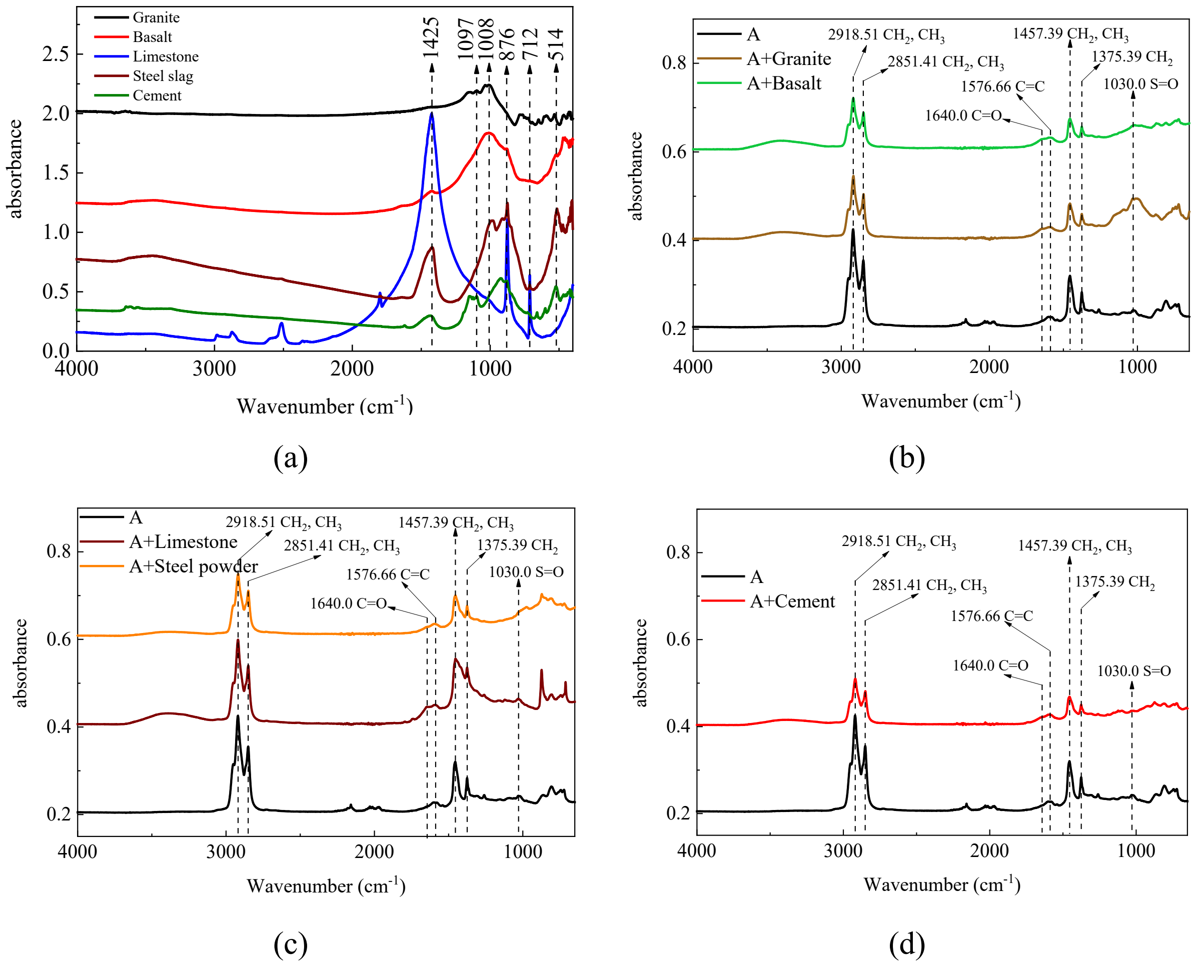

Figure 1. FTIR test results of (a) five fillers; (b) A+Granite and A+Basalt; (c) A+Limestone and A+Steel slag; (d) A+Cement

3.1.2. SEM test results

Figure 2 presents the SEM surface morphology of the fillers. From the figure, the granite particles have a smooth surface, a small specific surface area, and no apparent microporous structure, so it can be concluded that the surface morphology of granite has very limited benefits in terms of its adhesion ability to bitumen. As a comparison, the particle surface of the steel powder is rough and uneven, with rich folds and protrusions, which can effectively increase the bonding area between the bitumen and filler. Furthermore, many microporous structures are observed on the surface of steel powder particles, which means that components in bitumen easily penetrate the microporous structure of filler particles through the adsorption and capillarity, thus significantly improving the adhesion between the bitumen and steel powder filler. The surface morphology of the other three fillers (basalt, limestone, and cement) is between granite and steel powder. Combined with the above FTIR test results, it can be foreseen that the steel slag and cement will show better adhesion performance.

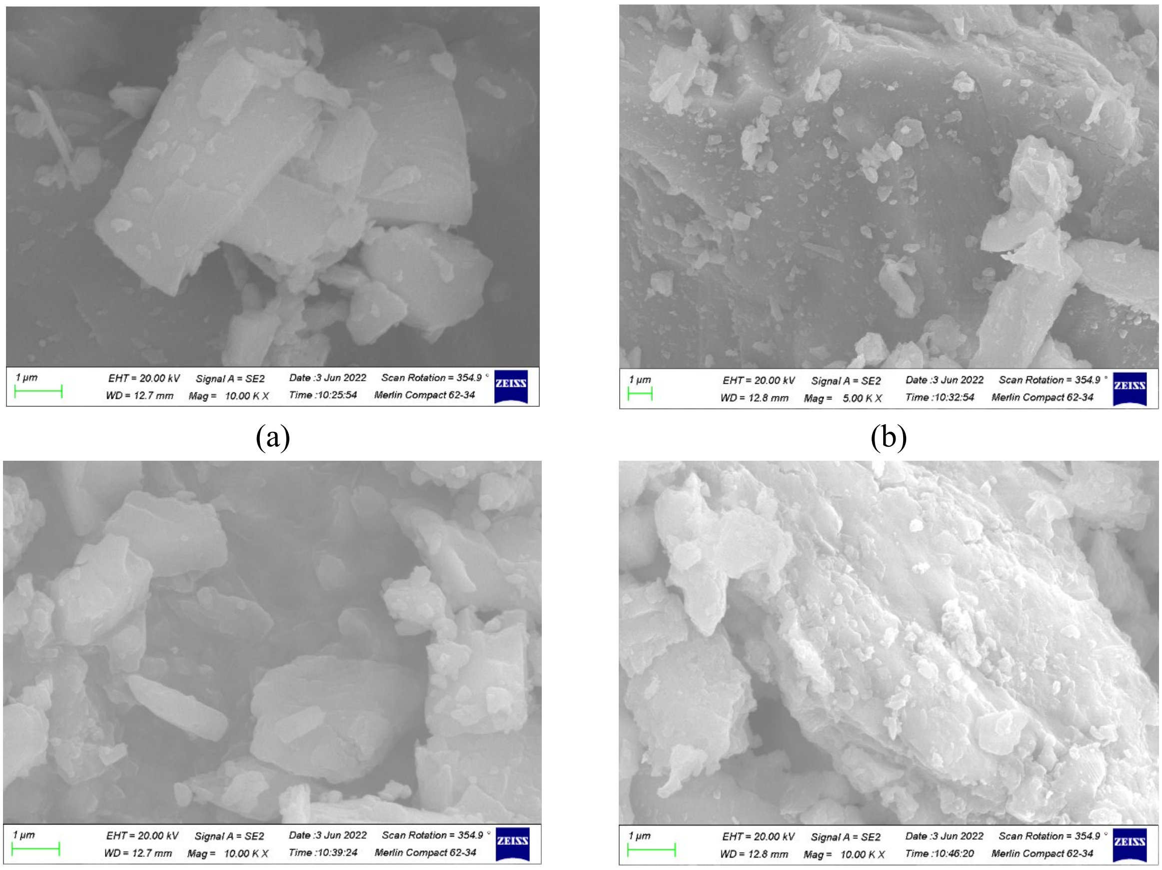

(a) (b) (c) (d)

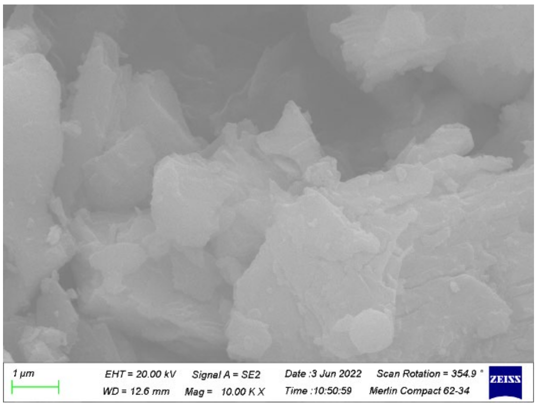

(e)

Figure 2. SEM surface morphology of fillers: (a) Granite; (b) Basalt; (c) Limestone; (d) Steel slag; (e) Cement

3.2. Macro test results

3.2.1. MSCR test results

Figure 3 shows the results of the average percent recovery (*R*) and non-recoverable creep compliance (J_{nr}) of the MSCR test of asphalt mastics under the two stress levels of 0.1kPa and 3.2kPa, respectively.

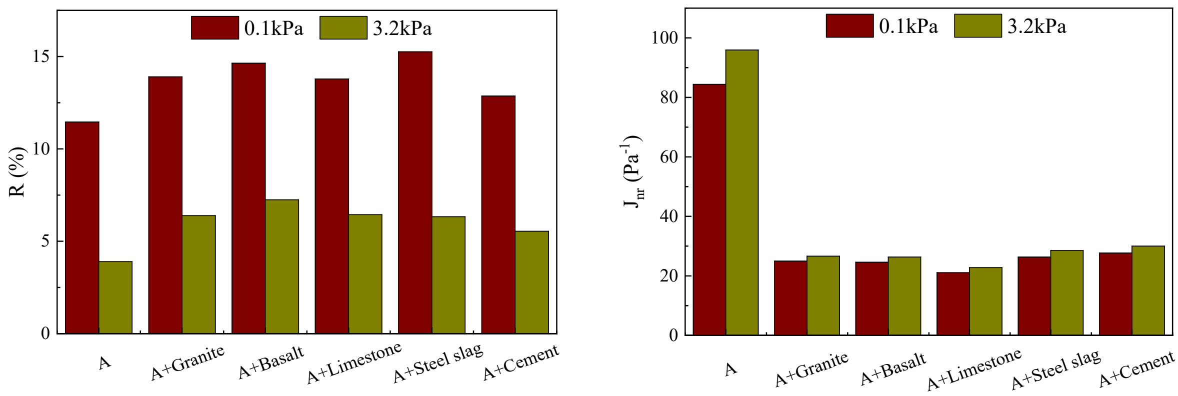

(a) (b)

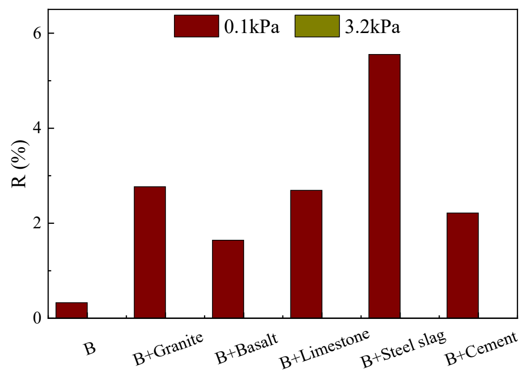
0.1kPa
3.2kPa
R (%)
B
B+Granite
B+Basalt
B+Limestone
B+Steel slag
B+Cement

(c)

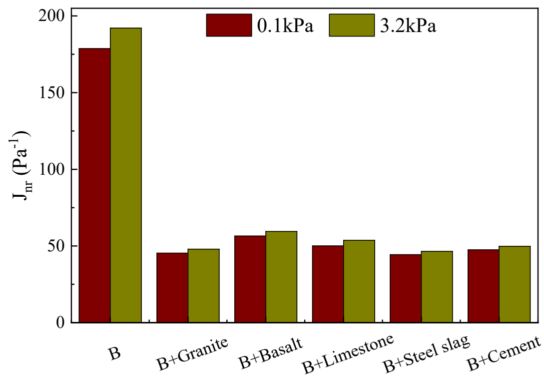
0.1kPa
3.2kPa
J_{nr} (Pa^{-1})
B
B+Granite
B+Basalt
B+Limestone
B+Steel slag
B+Cement

(d)

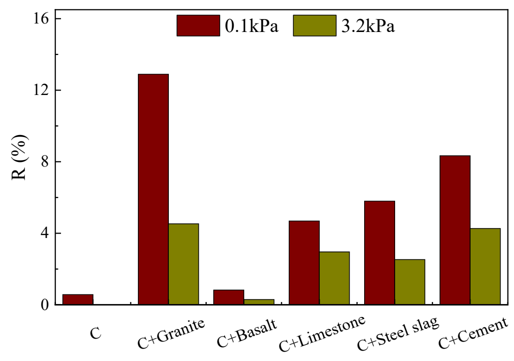
0.1kPa
3.2kPa
R (%)
C
C+Granite
C+Basalt
C+Limestone
C+Steel slag
C+Cement

(e)

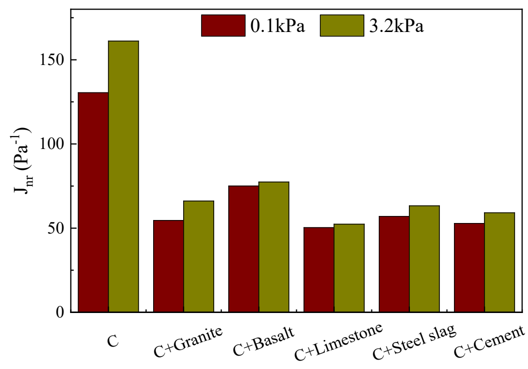
0.1kPa
3.2kPa
J_{nr} (Pa^{-1})
C
C+Granite
C+Basalt
C+Limestone
C+Steel slag
C+Cement

(f)

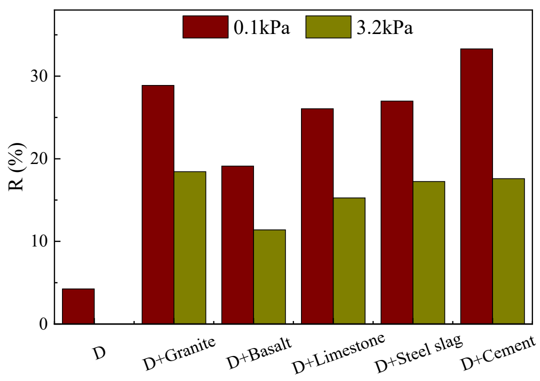
0.1kPa
3.2kPa
R (%)
D
D+Granite
D+Basalt
D+Limestone
D+Steel slag
D+Cement

(g)

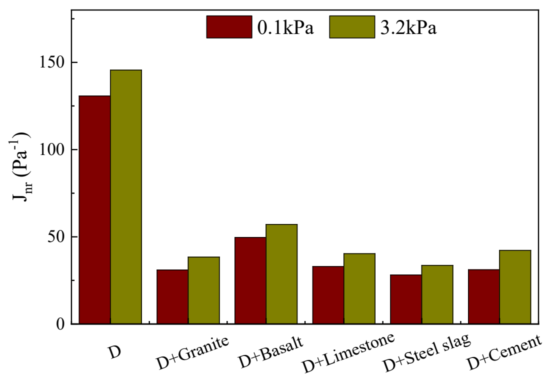
0.1kPa
3.2kPa
J_{nr} (Pa^{-1})
D
D+Granite
D+Basalt
D+Limestone
D+Steel slag
D+Cement

(h)

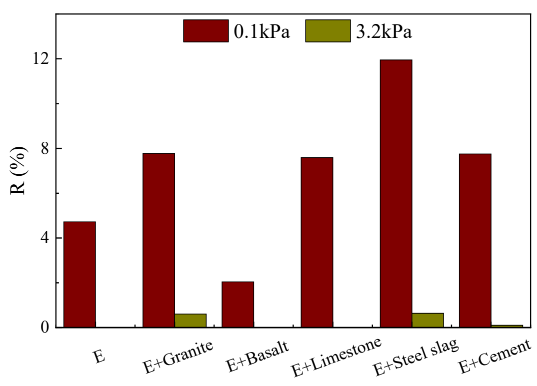
0.1kPa
3.2kPa
R (%)
E
E+Granite
E+Basalt
E+Limestone
E+Steel slag
E+Cement

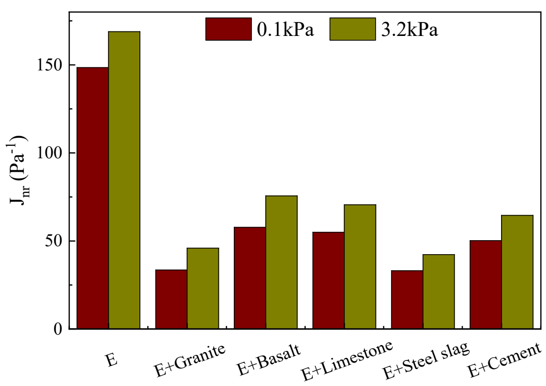
0.1kPa
3.2kPa
J_{nr} (Pa^{-1})
E
E+Granite
E+Basalt
E+Limestone
E+Steel slag
E+Cement

(i) (j)

Figure 3. MSCR test results of asphalt mastics: (a) R of A; (b) J_{nr} of A; (c) R of B; (d) J_{nr} of B; (e) R of C; (f) J_{nr} of C; (g) R of D; (h) J_{nr} of D; (i) R of E; (j) J_{nr} of E

The higher the R, the lower the J_{nr}, and the better the high-temperature damage resistance of asphalt mastics. Firstly, the MSCR test can clearly distinguish the high-temperature performance between different types of asphalt mastics based on the same bitumen matrix. As far as the five kinds of base bitumen in this study are concerned, among the five fillers, basalt has a minor enhancement on the high-temperature performance of the base bitumen in most cases. In addition, the enhancement effect of fillers on the base bitumen mainly manifests in the significant decrease of J_{nr}, while the increase in R is not substantial. This rule is shown in the other four base bitumen except for bitumen D.

3.2.2. LAS test results

Figure 4 presents the stress-strain curves of asphalt mastics. It can be seen from the figure that the peak stress of the stress-strain curves of asphalt mastics is significantly increased due to the addition of fillers. Among the five kinds of base bitumen, bitumen A, and bitumen C have the most significant increase, both of which can be increased from 4.0E5Pa to 1.2E6Pa. And the shapes of the stress-strain curves of different asphalt mastics based on the same bitumen matrix are similar. In addition, in the stress-strain curve, the strain corresponding to the peak stress represents the toughness of bituminous materials. The larger the strain value, the better the toughness of asphalt mastics. It can be seen intuitively that steel slag modified asphalt mastics has the strongest toughness among all asphalt mastics.

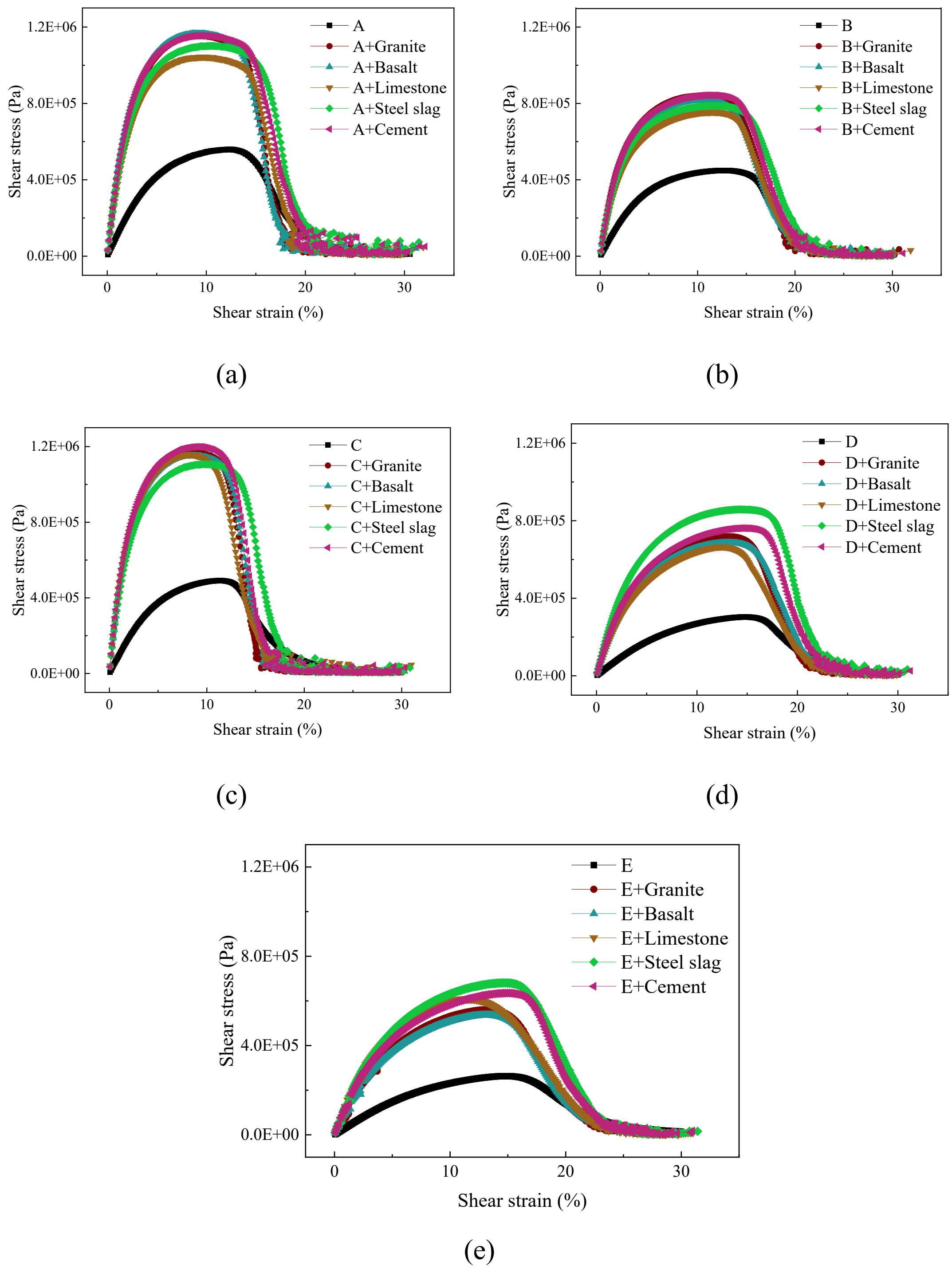

Figure 4. Stress-strain curves of asphalt mastics: (a) bitumen A; (b) bitumen B; (c) bitumen C; (d) bitumen D; (e) bitumen E

Figure 5 presents the integrity parameter curves of asphalt mastics, which describes the change of the integrity parameter with the damage integrity. The lower the integrity parameter, the more seriously the material is damaged. From the figures, the integrity parameter of bitumen is much higher than that of the asphalt mastic under the same damage integrity, which indicates that the use of fillers significantly weakens the fatigue damage properties of bitumen judging from the integrity parameters. In addition, there is no significant difference in the integrity parameter curves between the asphalt mastics based on the same bitumen matrix.

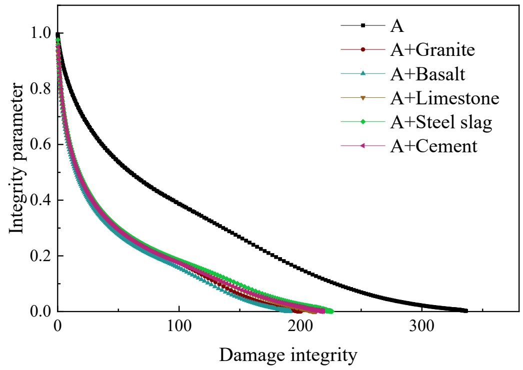

(a)

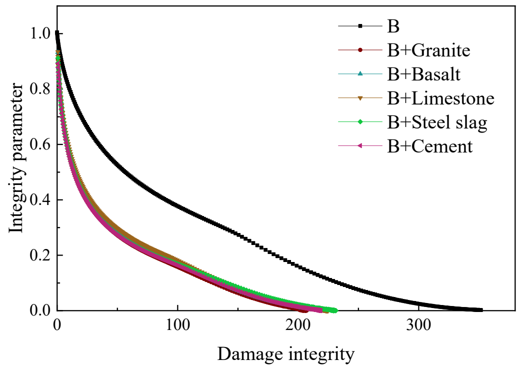

(b)

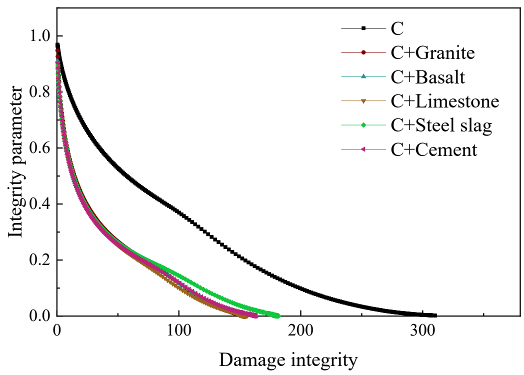

(c)

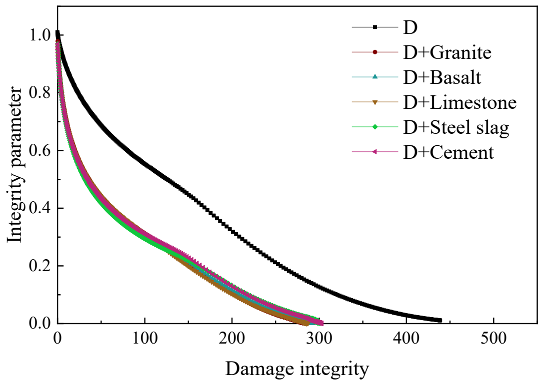

(d)

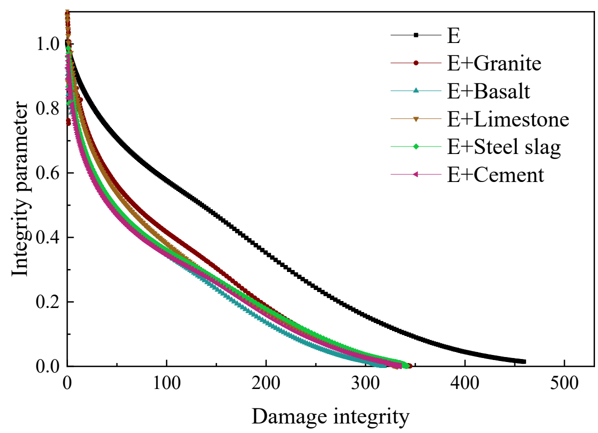

(e)

Figure 5. Damage integrity curves of asphalt mastics: (a) bitumen A; (b) bitumen B; (c) bitumen C; (d) bitumen D; (e) bitumen E

Figure 6 shows the fatigue life (N_f) of asphalt mastics at different strain levels. In addition to the two most used strain levels of 2.5% and 5% for the LAS test, two strain levels of 10% and 15% were added in this study. Firstly, the effect of fillers on the fatigue life of bitumen may be related to the strain level selected. Some fillers like steel slag and cement may extend the fatigue life of bitumen at low strain levels (2.5% and 5%), but the extension effect no longer exists when the strain level becomes larger (10% and 15%). In other words, the strain levels of 2.5% and 5% are problematic for computing the fatigue life of asphalt mastics whose modulus is much bigger than bitumen binder, which was also mentioned in a recent study by the research team that proposed the LAS test [37]. In addition, as far as the base bitumen used in this study is concerned, steel slag exhibits the strongest fatigue performance among the five asphalt mastics prepared from each base bitumen, followed by cement. At the same time, the other three types of fillers do not draw uniform rules in different base bitumen. In response to this phenomenon, this study interprets the effect of fillers on the fatigue performance of bitumen as the competitive mechanism between physical hardening and particle-filling enhancement. On the one hand, adding fillers increases the bitumen's modulus, making it brittle and weakening its fatigue properties. On the other hand, adding fillers has a reinforcing effect on bitumen. Specifically, with the decrease of the particle size and the increase of the specific surface area of the fillers, the number of interfaces between fillers and bitumen inside the asphalt mastic increases. Therefore, the asphalt mastic sample needs to destroy more filler-bitumen interfaces in the fatigue failure process; that is, the crack propagation path is more and longer, thus enhancing the fatigue life to a certain extent. This also explains why the steel slag and cement with the smaller particle size and the larger specific surface area significantly improve the fatigue life of bitumen.

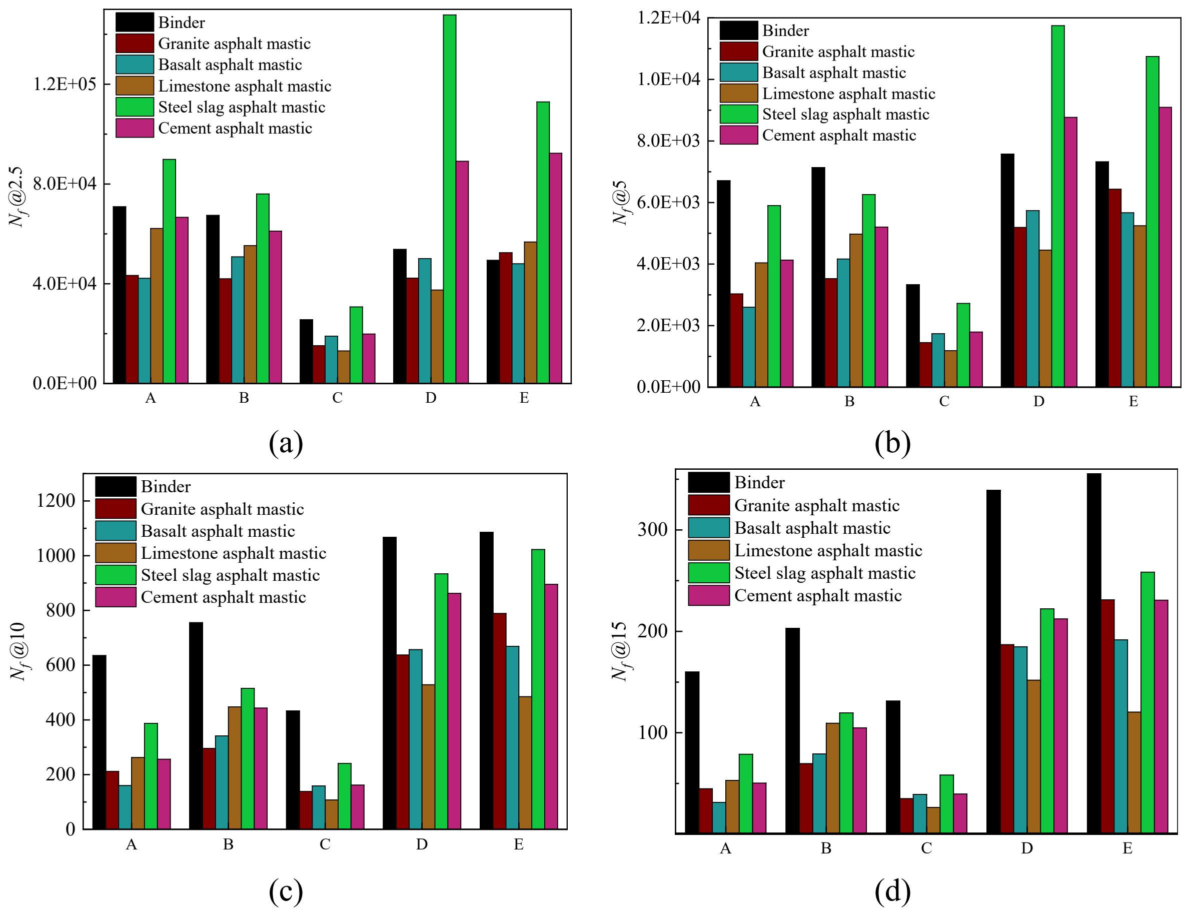

Figure 6. The fatigue life of asphalt mastics at different strain levels of (a) 2.5%; (b) 5%; (c) 10%; (d) 15%

3.2.3. BBR test results

Figure 7 shows the BBR test results of asphalt mastics, and the low-temperature PG of asphalt mastics was calculated based on the BBR test data and listed in Table 3. It is evident that the addition of all fillers significantly weakens the low-temperature cracking resistance of base bitumen. Among the five fillers, limestone and cement have the least negative effect on the low-temperature performance of base bitumen, which is the same among the five base bitumen used in this study. This may be due to the lower hardness of sedimentary rock (limestone) and cement compared with igneous rocks (granite and basalt) and steel slag, which leads to better low-temperature performance. In addition, it is worth noting that the BBR test only reflects the hardness and relaxation properties of bituminous materials. As mentioned above, the addition of fillers will improve the toughness of bitumen. To comprehensively evaluate the crack resistance of asphalt mastics, some tests characterizing the fracture toughness of materials, such as single-edge notch bending (SENB) [38] and double-edge-notched tension (DENT) tests [39], can be taken into consideration as the supplement of BBR test.

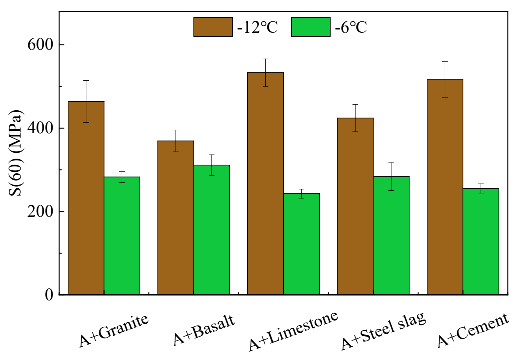

-12℃
-6℃
S(60) (MPa)
0
200
400
600
A+Granite
A+Basalt
A+Limestone
A+Steel slag
A+Cement

(a)

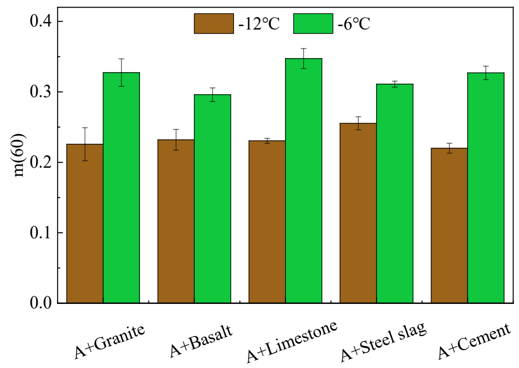

-12℃
-6℃
m(60)
0.0
0.1
0.2
0.3
0.4
A+Granite
A+Basalt
A+Limestone
A+Steel slag
A+Cement

(b)

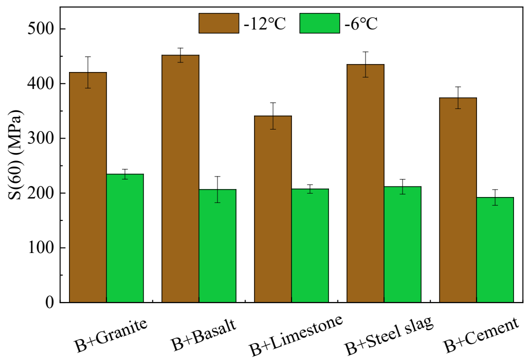

-12℃
-6℃
S(60) (MPa)
0
100
200
300
400
500
B+Granite
B+Basalt
B+Limestone
B+Steel slag
B+Cement

(c)

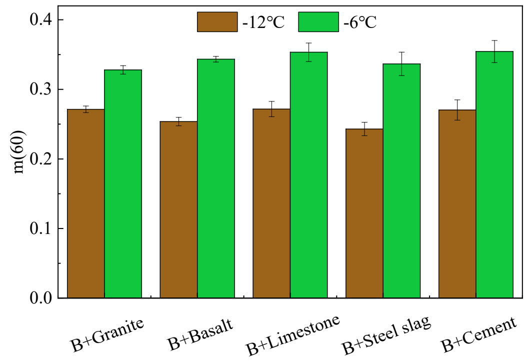

-12℃
-6℃
m(60)
0.0
0.1
0.2
0.3
0.4
B+Granite
B+Basalt
B+Limestone
B+Steel slag
B+Cement

(d)

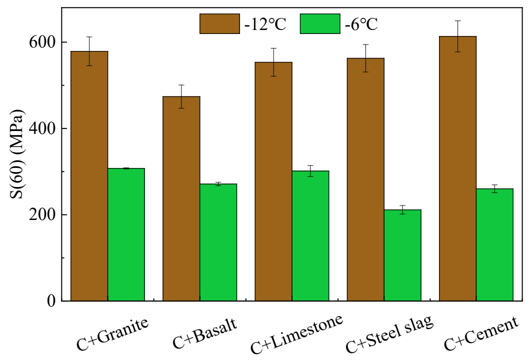

-12℃
-6℃
S(60) (MPa)
0
200
400
600
C+Granite
C+Basalt
C+Limestone
C+Steel slag
C+Cement

(e)

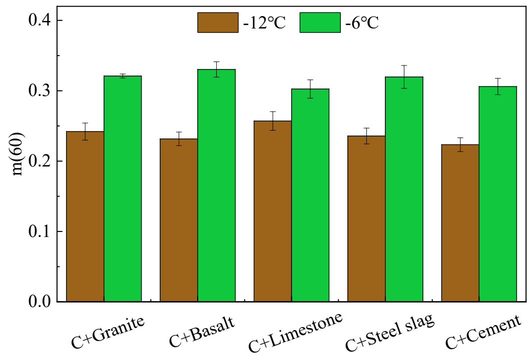

-12℃
-6℃
m(60)
0.0
0.1
0.2
0.3
0.4
C+Granite
C+Basalt
C+Limestone
C+Steel slag
C+Cement

(f)

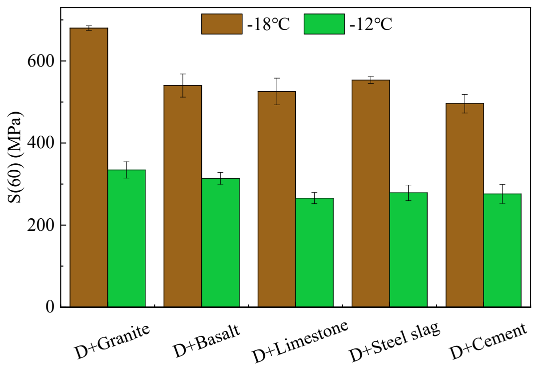

-18℃
-12℃
S(60) (MPa)
0
200
400
600
D+Granite
D+Basalt
D+Limestone
D+Steel slag
D+Cement

(g)

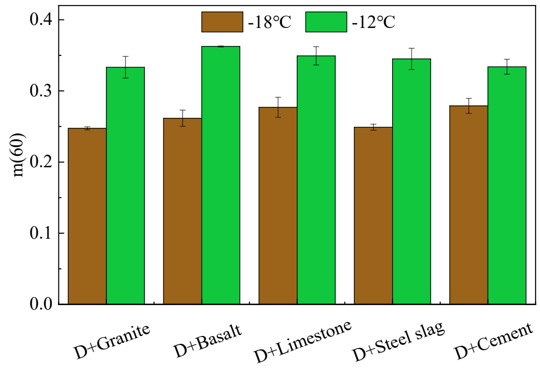

-18℃
-12℃
m(60)
0.0
0.1
0.2
0.3
0.4
D+Granite
D+Basalt
D+Limestone
D+Steel slag
D+Cement

(h)

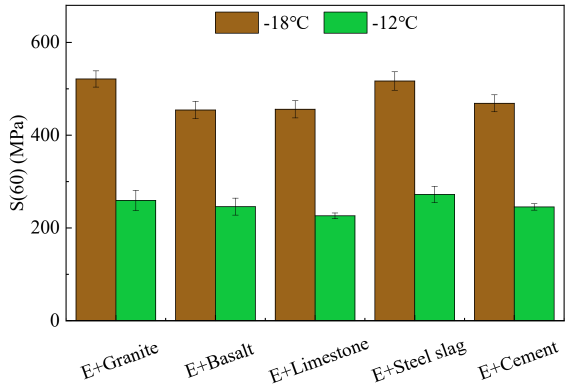

(i)

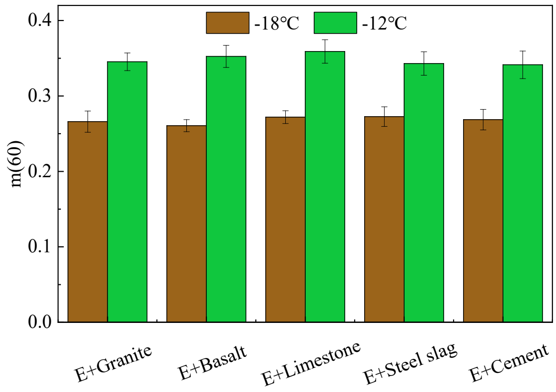

(j)

Figure 7. BBR test results of asphalt mastics: (a) *S* of A; (b) m-value of A; (c) *S* of B; (d) m-value of B; (e) *S* of C; (f) m-value of C; (g) *S* of D; (h) m-value of D; (i) *S* of E; (j) m-value of E

Table 3. Low-temperature PG of the asphalt mastics

Bitumen	Asphalt mastics	T_S (°C)	T_m (°C)	Low-temperature PG (°C)
A	A	-27.55	-26.98	-26.98
	A+Granite	-16.72	-17.61	-16.72
	A+Basalt	-14.68	-15.63	-14.68
	A+Limestone	-17.64	-18.91	-17.64
	A+Steel slag	-16.83	-15.86	-15.86
	A+Cement	-17.37	-17.74	-17.37
B	B	-27.38	-22.00	-22.00
	B+Granite	-18.53	-18.96	-18.53
	B+Basalt	-18.86	-18.90	-18.86
	B+Limestone	-19.65	-19.92	-19.65
	B+Steel slag	-18.90	-18.35	-18.35
	B+Cement	-20.01	-19.88	-19.88
C	C	-26.63	-21.85	-21.85
	C+Granite	-15.76	-17.59	-15.76

	C+Basalt	-20.92	-20.16	-20.16
	C+Limestone	-22.05	-21.67	-21.67
	C+Steel slag	-19.86	-20.60	-19.86
	C+Cement	-21.01	-21.56	-21.01
D	D	-30.25	-29.41	-29.41
	D+Granite	-21.08	-24.33	-21.08
	D+Basalt	-21.49	-25.72	-21.49
	D+Limestone	-23.07	-26.09	-23.07
	D+Steel slag	-22.65	-24.81	-22.65
	D+Cement	-22.86	-25.71	-22.86
E	E	-30.72	-30.72	-30.72
	E+Granite	-23.25	-25.43	-23.25
	E+Basalt	-23.94	-25.43	-23.94
	E+Limestone	-24.42	-26.07	-24.42
	E+Steel slag	-22.91	-25.67	-22.91
	E+Cement	-23.92	-25.87	-23.92

3.2.4. Boiling water test results

Figure 8 presents the peeling rate results of asphalt mastics. From the figures, granite modified asphalt mastics show the worst adhesion performance, followed by basalt modified asphalt mastics. In contrast, cement modified asphalt mastics exhibit the best adhesion performance, followed by steel slag modified asphalt mastics and limestone modified asphalt mastics. Among the five kinds of base bitumen used in this study, the ranking of adhesion performance between five asphalt mastics is consistent, which verifies the analysis conclusions of the microscopic test results above.

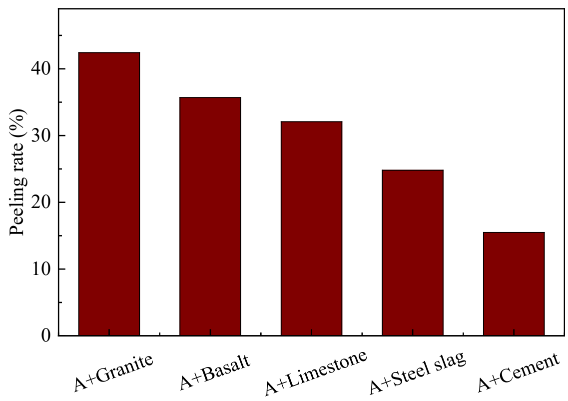

(a)

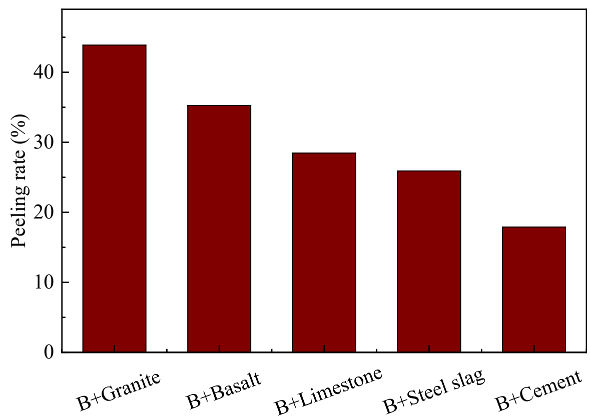

(b)

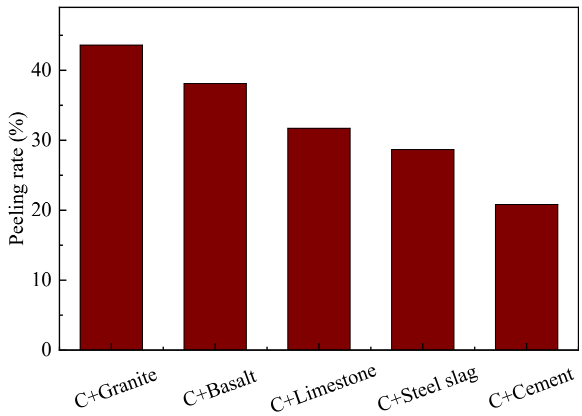

(c)

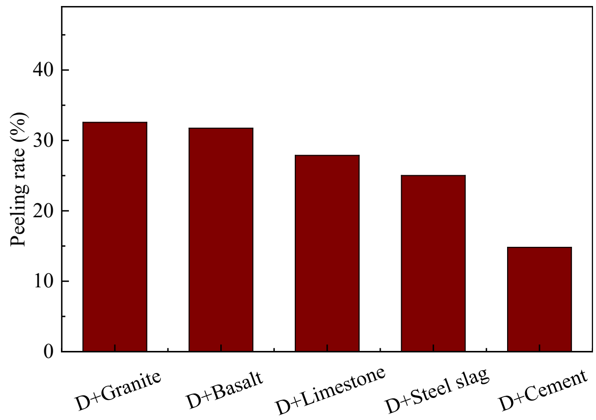

(d)

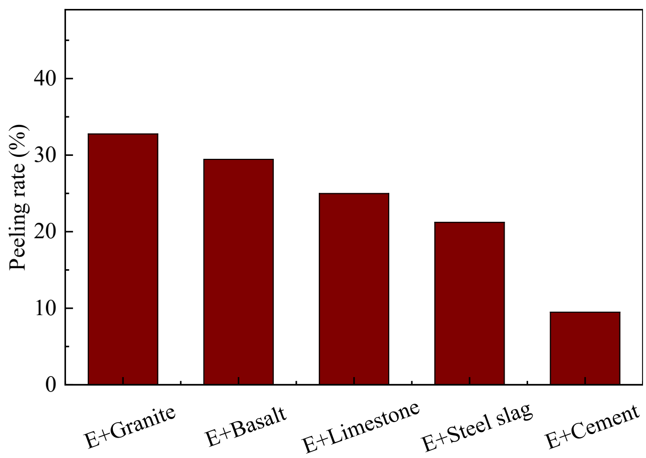

(e)

Figure 8. Peeling rate of asphalt mastics: (a) bitumen A; (b) bitumen B; (c) bitumen C; (d) bitumen D; (e) bitumen E

3.3. Results of GRA

3.3.1. GRA results of high-temperature performances

Since the use of fillers does not significantly affect the *R* of asphalt mastics, the J_{nr} at the two stress levels of 0.1kPa and 3.2kPa was selected as the parameters reflecting the high-temperature performance of asphalt mastics in this study. Figure 9 presents the grey relational grades between the high-temperature indexes and the raw material characteristics (including components and penetrations of bitumen and filler characteristics). It can be seen from the figures that the penetrations of bitumen properties, and fineness parameters (D10 and D90) and P20 of filler characteristics are the most significant factors affecting the high-temperature performance of asphalt mastics. This study adopted the same criteria as the literature [33], stating that when the grey correlation degree is greater than 0.75, it indicates a substantial correlation between the raw material characteristics and the performances of asphalt mastics. In the GRA results of $J_{nr\text{-}0.1}$ and $J_{nr\text{-}3.2}$, the correlation degrees of D10, penetrations, D90 and P20 are the highest, all of which are greater than 0.75 and followed by some bitumen components (asphaltene and aromatics), as well as the SSA and D50 of the fillers. In addition, the mineral powder composition of the fillers (SiO_2 and CaO) is the least influential factor among all raw material characteristics. Moreover, it is worth mentioning that, compared with P5 and P10, the correlation between P20 and J_{nr} is significantly higher than that of the former two. To conclude, the high-temperature performance of the mastics mainly depends on the fineness parameters (D10 and D90) of the fillers and the penetrations of bitumen. Besides, the content of fillers with a diameter of less than 0.02 mm (P20) is also a critical parameter affecting the high-temperature performance.

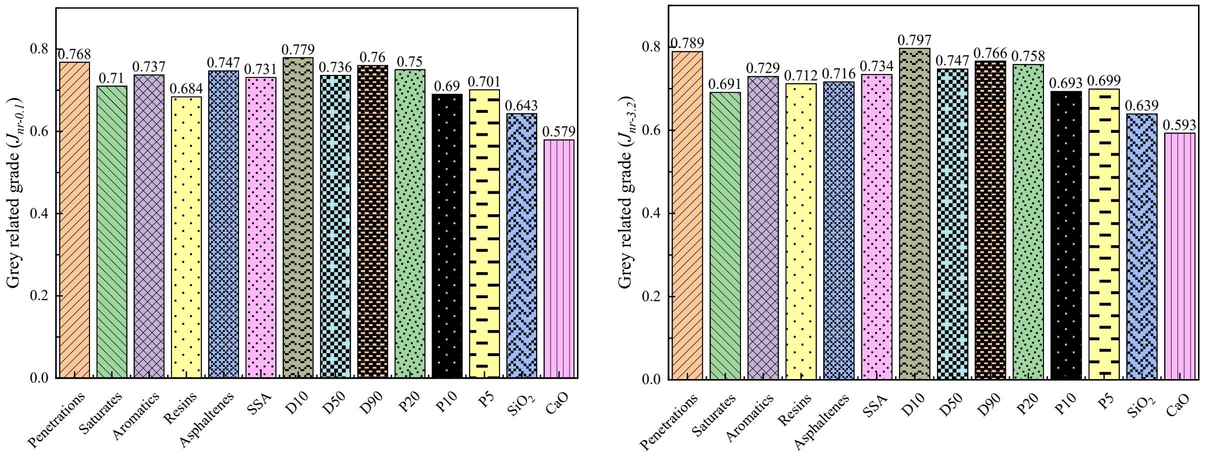

(a) (b)

Figure 9. Grey relational grades between the high-temperature indexes and the raw material characteristics: (a) $J_{nr-0.1}$; (b) $J_{nr-3.2}$

3.3.2. GRA results of medium-temperature performances

Figure 10 presents the grey relational grades between the medium-temperature indexes (N_f at four strain levels of 2.5%, 5%, 10%, and 15%) and the raw material characteristics. From the figures, when N_f is at a low strain level (2.5%), the SSA and P20 of fillers have the most significant impact on the fatigue performance of the mastics, followed by P5 and P10, and the next are the aromatics and resins contents, and penetrations of bitumen. In other words, at low strain levels, the fatigue performance of the mastics mainly depends on the SSA and small particle proportion parameters (P20, P5, and P10) of fillers. When the strain level was increased (5%, 10%, and 15%), the resins content of bitumen was the most remarkable factor affecting the fatigue performance of the mastics, followed by SSA of the filler, the small particle proportion parameters (P20, P10, and P5) and the fineness parameters (D10, D50, and D90). To sum up, to achieve a better fatigue performance of asphalt mastics, the key is controlling the resin content of bitumen and the SSA and fineness of fillers.

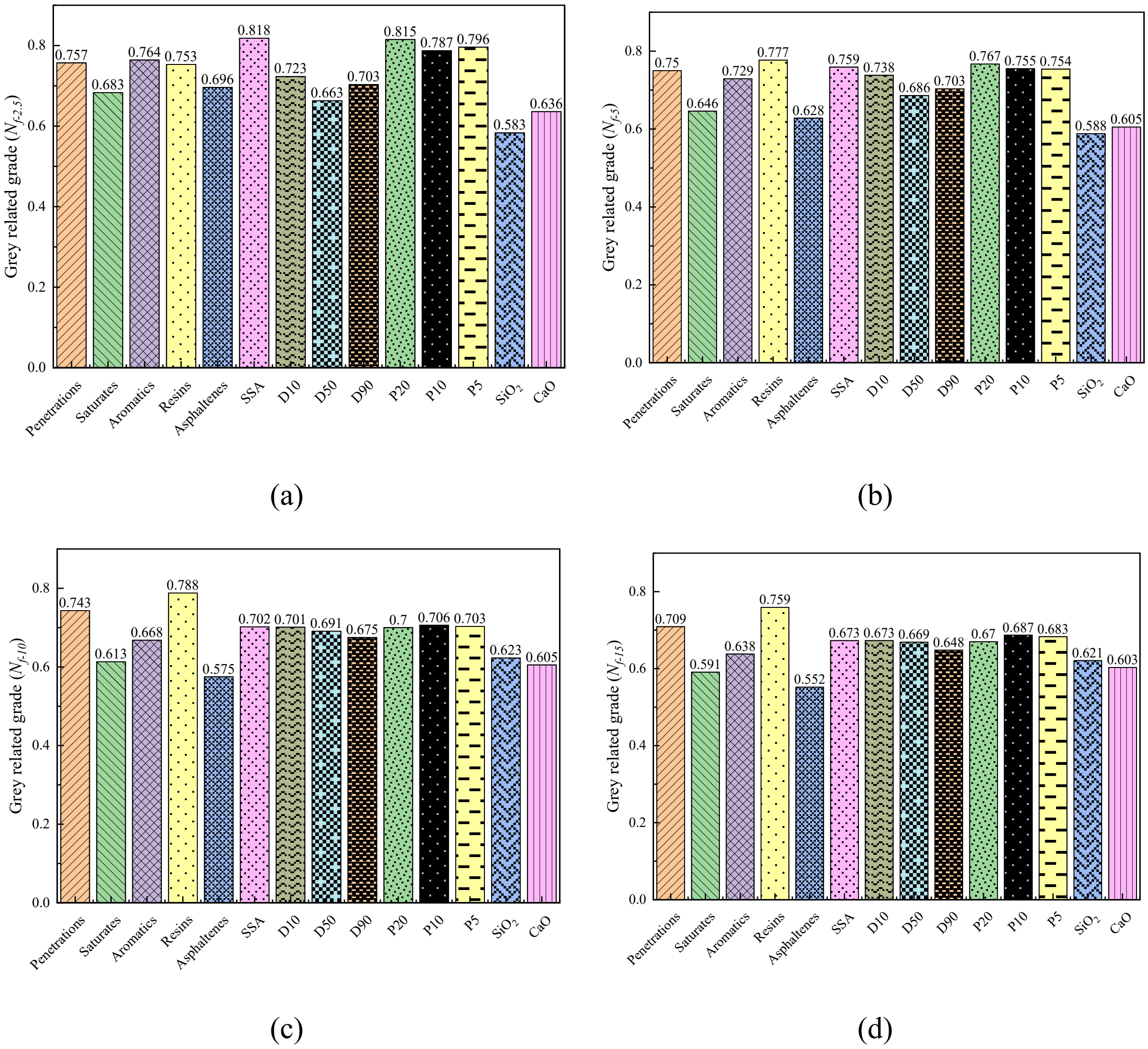

Figure 10. Grey relational grades between the medium-temperature indexes and the raw material characteristics: (a) $N_{f-2.5}$; (b) N_{f-5}; (c) N_{f-10}; (d) N_{f-15}

3.3.3. GRA results of low-temperature performances

Figure 11 presents the grey relational grades between the low-temperature indexes (T_S and T_m) and the raw material characteristics. It can be found from the figure the penetrations of bitumen were the most significant factor affecting the low-temperature performance of the mastics. D10 and P20 are the two factors most closely related to the low-temperature properties among the filler characteristics. These are followed by the SSA of fillers and resin content of bitumen, followed by D90 and the aromatics content of bitumen. Among all the raw material characteristics, the mineral composition of fillers (CaO and SiO_2) was the least relevant factor, which is also consistent with the previous results. To summarize, the low-temperature performance of asphalt mastics mainly depends on penetrations of bitumen, and some characteristics of fillers such as D10, P20, and SSA. Moreover, the resin content of bitumen also has a high contribution to the low-temperature performance.

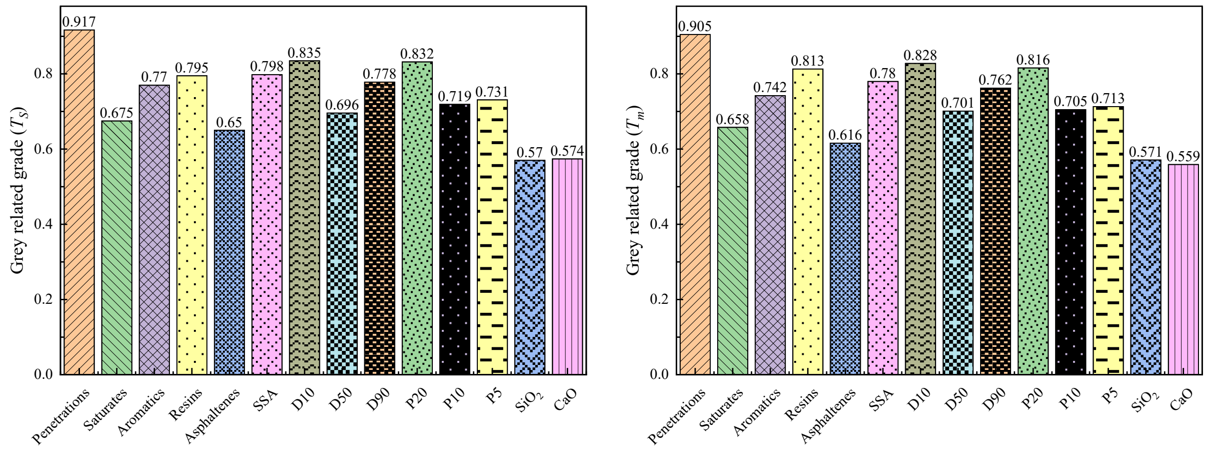

(a) (b)

Figure 11. Grey relational grades between the low-temperature indexes and the raw material characteristics: (a) T_S; (b) T_m

3.3.4. GRA results of adhesion performances

Figure 12 presents the grey relational grades between the adhesion index (peeling rate) and the raw material characteristics. As we can find in the figure, the fineness parameters of the filler (D10, D50, and D90) are the most influential factors in the moisture resistance of asphalt mastics. Followed by penetrations, and aromatics and asphaltenes contents of bitumen, and next is P20 of fillers. Furthermore, it is worth mentioning that the gray correlation degree of D10 is much higher than other factors. It is not difficult to conclude that the adhesion performance of mastics mainly depends on the fineness parameter of the filler.

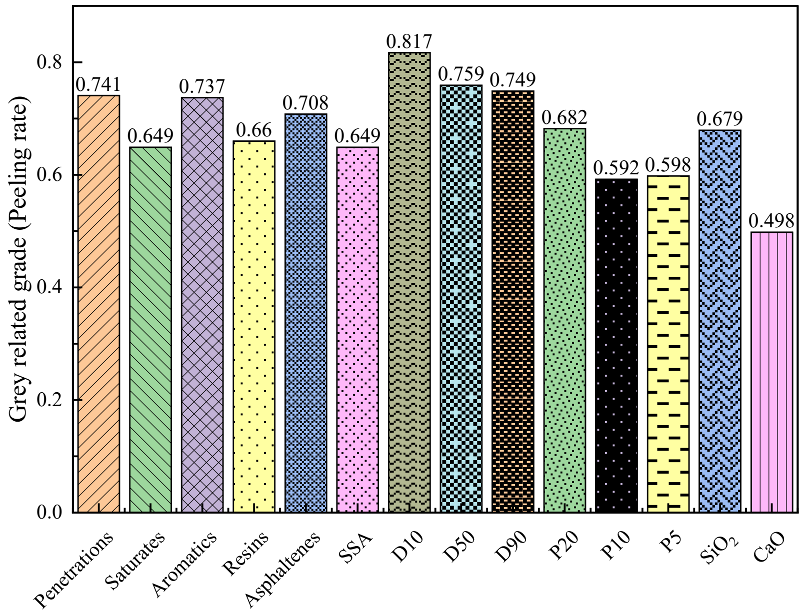

Figure 12. Grey relational grades between the adhesion index and the raw material characteristics

4. Conclusions and outlook

The current study focuses on the compatibility between bitumen and fillers. Both macro and micro tests were carried out on the asphalt mastics, and the grey relational analysis was conducted to investigate the relationship between raw material characteristics and performances of asphalt mastics. The major conclusion from this study includes:

(1) In general, the properties of asphalt mastics, such as high temperature, fatigue, low temperature, and adhesion, exhibit a high correlation with the raw material characteristics. Asphalt mastics can achieve better performance by controlling the bitumen components and filler characteristics such as fineness, specific surface area (SSA), and small particle composition content.

(2) The resin content of bitumen is suggested to be one of the most influential properties on the fatigue performance of asphalt mastics. With the increase in strain levels, the difference between the gray correlation degree of resins and that of other factors is more significant. In addition, the contents of resins and aromatics also exhibit a specific contribution to the low-temperature performance of asphalt mastics.

(3) D10 of filler has the highest correlation with the high-temperature, low-temperature, and adhesion performance of asphalt mastics. P20 of the filler also shows a relatively high correlation in these properties of mastics. Furthermore, these two parameters exhibit a higher correlation than similar parameters (D50, D90, P10, and P5). Therefore, D10 and P20 are recommended as two critical indicators for selecting fillers.

(4) The filler characteristics such as fineness and SSA will significantly affect the fatigue performance of asphalt mastics because the effect of fillers on the fatigue performance of mastics is the competitive mechanism between physical hardening and particle-filling enhancement. The filler with small particle size and large SSA can prolong and increase the propagation path of fatigue cracks, thus effectively improving the fatigue performance of asphalt mastics.

This study investigates the effects of bitumen components and filler characteristics on various performances of asphalt mastics only from the perspective of raw materials. In the future study, further research will be conducted to achieve precise control and prediction of the performance of mastics, such as characterization of the contribution of the physical and chemical interaction between bitumen and filler to the performance of mastics, and study of the interaction between bitumen and filler from the molecular dynamics (MD) scale.

Acknowledgments

The work underlying this project was financially supported by the National Key Research and Development Program of China (2019YFE0116300), the National Natural Science Foundation of China (52250610218), and the Natural Science Foundation of Heilongjiang Province of China (JJ2020ZD0015). The authors gratefully acknowledge their financial support.

Disclosure statement

The authors disclosed no potential conflicts of interest.

References

[1] J. Xu, B. Hong, G. Lu, T. Li, S. Wang, C. Wang, D. Wang, Carboxylated styrene-butadiene latex (XSB) in asphalt modification towards cleaner production and enhanced performance of pavement in cold regions, Journal of Cleaner Production 372 (2022) 133653.

[2] Z. Fan, J. Lin, Z. Chen, P. Liu, D. Wang, M. Oeser, Multiscale understanding of interfacial behavior between bitumen and aggregate: From the aggregate mineralogical genome aspect, Construction and Building Materials 271 (2021) 121607.

[3] M. Kim, G. Buttlar William, Differential Scheme Effective Medium Theory for Hot-Mix Asphalt E* Prediction, Journal of Materials in Civil Engineering 23(1) (2011) 69-78.

[4] Q. Gu, A. Kang, B. Li, P. Xiao, H. Ding, Effect of fiber characteristic parameters on the high and low temperature rheological properties of basalt fiber modified asphalt mortar, Case Studies in Construction Materials 17 (2022) e01247.

[5] A. Rahim, A. Milad, N.I. Yusoff, G. Airey, N. Thom, Stiffening Effect of Fillers Based on Rheology and Micromechanics Models, Applied Sciences, 2021.

[6] B.S. Underwood, Y.R. Kim, A four phase micro-mechanical model for asphalt mastic modulus, Mechanics of Materials 75 (2014) 13-33.

[7] X. Zhu, Z. Du, H. Ling, L. Chen, Y. Wang, Effect of filler on thermodynamic and mechanical behaviour of asphalt mastic: a MD simulation study, International Journal of Pavement Engineering 21(10) (2020) 1248-1262.

[8] J. Zhang, X. Li, G. Liu, J. Pei, Effects of material characteristics on asphalt and filler interaction ability, International Journal of Pavement Engineering 20(8) (2019) 928-937.

[9] F. Li, Y. Yang, L. Wang, Evaluation of physicochemical interaction between asphalt binder and mineral filler

through interfacial adsorbed film thickness, Construction and Building Materials 252 (2020) 119135.

[10] H.M. Yin, W.G. Buttlar, G.H. Paulino, H.D. Benedetto, Assessment of Existing Micro-mechanical Models for Asphalt Mastics Considering Viscoelastic Effects, Road Materials and Pavement Design 9(1) (2008) 31-57.

[11] Y. Cheng, J. Tao, Y. Jiao, G. Tan, Q. Guo, S. Wang, P. Ni, Influence of the properties of filler on high and medium temperature performances of asphalt mastic, Construction and Building Materials 118 (2016) 268-275.

[12] M. Nazary, S. Kofteci, Effect of filler types and asphalt penetration grade on properties of asphalt mastic, Petroleum Science and Technology 36(18) (2018) 1503-1509.

[13] N.A. Mohd Shukry, N. Abdul Hassan, M.E. Abdullah, M.R. Hainin, N.I.M. Yusoff, M.Z.H. Mahmud, R. Putra Jaya, M.N.M. Warid, Mohd K.I. Mohd Satar, Influence of diatomite filler on rheological properties of porous asphalt mastic, International Journal of Pavement Engineering 21(4) (2020) 428-436.

[14] S. Li, F. Ni, Q. Dong, Z. Zhao, X. Ma, Effect of filler in asphalt mastic on rheological behaviour and susceptibility to rutting, International Journal of Pavement Engineering 22(1) (2021) 87-96.

[15] J. Jiang, Y. Zhao, G. Lu, Y. Dai, F. Ni, Q. Dong, Effect of binder film distribution on the fatigue characteristics of asphalt Binder/Filler composite based on image analysis method, Construction and Building Materials 260 (2020) 119876.

[16] Y. Tan, M. Guo, Micro- and Nano-Characteration of Interaction Between Asphalt and Filler, Journal of Testing and Evaluation 42(5) (2014) 1089-1097.

[17] Q. Zhang, Z. Huang, Investigation of the Microcharacteristics of Asphalt Mastics under Dry–Wet and Freeze–Thaw Cycles in a Coastal Salt Environment, Materials, 2019.

[18] W. Xu, X. Qiu, S. Xiao, H. Hong, F. Wang, J. Yuan, Characteristics and Mechanisms of Asphalt–Filler Interactions from a Multi-Scale Perspective, Materials, 2020.

[19] F. Li, Y. Yang, Experimental investigation on the influence of interfacial effects of limestone and fly ash filler particles in asphalt binder on mastic aging behaviors, Construction and Building Materials 290 (2021) 123184.

[20] R. Moraes, H.U. Bahia, Effect of mineral filler on changes in molecular size distribution of asphalts during oxidative ageing, Road Materials and Pavement Design 16(sup2) (2015) 55-72.

[21] B. Xing, C. Qian, H. Sun, J. Che, Y. Lyu, Reliability study on rheological and cracking behavior of mastics using different sized particles, Advanced Powder Technology 32(6) (2021) 2029-2042.

[22] B. Xing, W. Fan, L. Han, C. Zhuang, C. Qian, X. Lv, Effects of filler particle size and ageing on the fatigue behaviour of bituminous mastics, Construction and Building Materials 230 (2020) 117052.

[23] M. Guo, Y. Tan, J. Yu, Y. Hou, L. Wang, A direct characterization of interfacial interaction between asphalt binder and mineral fillers by atomic force microscopy, Materials and Structures 50(2) (2017) 141.

[24] H.R. Fischer, E.C. Dillingh, C.G.M. Hermse, On the interfacial interaction between bituminous binders and mineral surfaces as present in asphalt mixtures, Applied Surface Science 265 (2013) 495-499.

[25] C. Li, Z. Chen, S. Wu, B. Li, J. Xie, Y. Xiao, Effects of steel slag fillers on the rheological properties of asphalt mastic, Construction and Building Materials 145 (2017) 383-391.

[26] Q. Li, Y. Qiu, A. Rahman, H. Ding, Application of steel slag powder to enhance the low-temperature fracture properties of asphalt mastic and its corresponding mechanism, Journal of Cleaner Production 184 (2018) 21-31.

[27] K.-z. Yan, H.-b. Xu, H.-l. Zhang, Effect of mineral filler on properties of warm asphalt mastic containing Sasobit, Construction and Building Materials 48 (2013) 622-627.

[28] D. Movilla-Quesada, A.C. Raposeiras, D. Castro-Fresno, D. Peña-Mansilla, Experimental study on stiffness development of asphalt mixture containing cement and Ca(OH)2 as contribution filler, Materials & Design 74

(2015) 157-163.
[29] M.-C. Liao, G. Airey, J.-S. Chen, Mechanical Properties of Filler-Asphalt Mastics, International Journal of Pavement Research and Technology 6(5) (2013) 576-581.
[30] K.R. Usman, M.R. Hainin, M.K.I.M. Satar, M.N.M. Warid, A. Usman, Z.H. Al-Saffar, M.A. Bilema, A comparative assessment of the physical and microstructural properties of waste garnet generated from automated and manual blasting process, Case Studies in Construction Materials 14 (2021) e00474.
[31] J. Zhang, L.F. Walubita, A.N.M. Faruk, P. Karki, G.S. Simate, Use of the MSCR test to characterize the asphalt binder properties relative to HMA rutting performance – A laboratory study, Construction and Building Materials 94 (2015) 218-227.
[32] M. Sabouri, D. Mirzaiyan, A. Moniri, Effectiveness of Linear Amplitude Sweep (LAS) asphalt binder test in predicting asphalt mixtures fatigue performance, Construction and Building Materials 171 (2018) 281-290.
[33] B. Li, P. Liu, Y. Zhao, X. Li, G. Cao, Effect of graphene oxide in different phases on the high temperature rheological properties of asphalt based on grey relational and principal component analysis, Construction and Building Materials 362 (2023) 129714.
[34] M. Gong, H. Zhang, B. Yang, Q. Sun, Analysis of the influencing factors on the anti-aging performance of a hybrid-modified asphalt mixture using the grey relational theory, International Journal of Pavement Engineering 22(5) (2021) 597-612.
[35] Y.-R. Kim, I. Pinto, S.-W. Park, Experimental evaluation of anti-stripping additives in bituminous mixtures through multiple scale laboratory test results, Construction and Building Materials 29 (2012) 386-393.
[36] D. Fee, R. Maldonado, G. Reinke, H. Romagosa, Polyphosphoric Acid Modification of Asphalt, Transportation Research Record 2179(1) (2010) 49-57.
[37] H. Chen, H.U. Bahia, Modelling effects of aging on asphalt binder fatigue using complex modulus and the LAS test, International Journal of Fatigue 146 (2021) 106150.
[38] R. Velasquez, H. Tabatabaee, H. Bahia, Low Temperature Cracking Characterization of Asphalt Binders by Means of the Single-Edge Notch Bending (SENB) Test, Journal of the Association of Asphalt Paving Technologists 80 (2011).
[39] J. Xu, Z. Guo, G. Lu, Z. Fan, D. Wang, M. Oeser, Reclamation of waste oils in asphalt modification towards enhanced low-temperature performance of pavement in cold region, International Journal of Pavement Engineering (2022) 1-16.